View metadata, citation and similar papers at core.ac.uk
brought to you by CORE
provided by CERN Document Server

Simulation of a Space-Based Microlensing Survey for Terrestrial Extra-Solar Planets

David P. Bennett & Sun Hong Rhie

Department of Physics, University of Notre Dame, Notre Dame, IN 46556

email: bennett@nd.edu, srhie@nd.edu

ABSTRACT

The gravitational microlensing technique can be used to carry out a sensitive survey of planets ranging in mass from giant planets down to Mars-mass planets. This requires photometric monitoring of a large number of stars ($\sim 10^8$) with high angular and temporal resolution. The Galactic Exoplanet Survey Telescope (GEST) is a 1.5m space based telescope with a large field-of-view that has recently been submitted to NASA's Discovery competition to carry out such a extra-solar planet search survey. We present a simulation of the baseline GEST mission, and we use this simulation to determine GEST's extra-solar planet detection sensitivity. We find that GEST will be sensitive to planets down to the mass of Mars, and will detect 100 Earth-mass planets at 1 AU if every star has such a planet. GEST's highest sensitivity is at separations of 0.7-10 AU, but it will also have significant sensitivity at larger separations and will be able to detect free-floating planets in significant numbers. GEST will also be able to detect $\sim 50,000$ giant planets via transits, and it is, therefore, the only proposed planet detection method that is sensitive to planets at all orbital radii.

An important strength of the gravitational microlensing technique is that low-mass planets can be detected with high signal-to-noise, and we find that GEST can detect Earth-mass planets with a typical significance level of nearly 30σ. This means that the planetary signals are strong enough so that there is no confusion between planetary microlensing signals and other types of perturbations to the microlensing light curves.

Subject headings: dark matter - gravitational lensing

1. Introduction

The discovery of the first extra-solar planets a few years ago (Mayor & Queloz 1995; Marcy & Butler 1996; Butler & Marcy 1996) has spurred the growth of a new branch of observational astronomy, the study of extra-solar planets. The success of the precision radial velocity technique has been spectacular (Marcy, Cochran & Mayor 2000; Perryman 2000; Marcy & Butler 2000) with the discovery of more than 50 extra-solar giant planets in the past six years. This technique is sensitive enough to detect Jupiter-mass planets in Jupiter-like orbits, and it is anticipated that such planets will be discovered in the next few years as the duration of the radial velocity monitoring programs approaches Jupiter's orbital period of 12 years. The dramatic success of these radial velocity extra-solar planet search programs has encouraged the astronomical community to address the far more ambitious goal of searching for Earth-like extra-solar planets (Dressler et al. 2000) because such planets seem best suited for life. The search for Earth-like extra-solar planets has now become a major NASA goal. It is likely that it will require the development of new extra-solar planet search techniques since it is thought that the intrinsic radial velocity noise of stars will limit this technique to planets with masses $\gtrsim$ a few $\times 10^{-4}$ of the host star's mass which is 100 times greater than an Earth mass.

A number of extra-solar planet search methods have been proposed that should be able to detect planets in the Earth mass range (Perryman 2000). The most ambitious of these are the Terrestrial Planet Finder (TPF) (Beichman 1998) and Darwin (Fridlund 2000) missions which will have the ability to directly detect Earth-like planets around nearby stars. However, these missions require a considerable amount of technological development before it will be ready to fly. The Space Interferometry Mission (SIM) (Danner & Unwin 1999) is a pre-cursor to TPF which will be able to detect planets of a few Earth masses around nearby stars via their astrometric effects on the stars they orbit. But, SIM also requires some technical development before it will be ready to fly.

The gravitational microlensing and transit techniques are two methods that should have sensitivity to terrestrial planets, but are technically easier than SIM or TPF. These missions are sensitive to planets orbiting distant stars, so they are most useful for obtaining statistical information regarding the abundance of planetary systems. The transit technique is employed by the COROT mission (Schneider et al. 1998) which is slated for launch by CNES in 2004, the Eddington mission (Deeg et al. 2000) which has recently been selected as an ESA F2/F3 "reserve" mission, and Kepler mission (Koch et al. 1998) which is being considered by NASA's Discovery Program. However, these surveys share the property that the transit signal due to an Earth-like planet is a photometric variation of only $\sim 0.01\,\%$ which is only slightly above the anticipated photometric noise.

The gravitational microlensing technique (Mao & Paczynski 1991; Gould & Loeb 1992; Bennett et al. 2000), has the unique property that the strength of the planet's photometric microlensing signal is nearly independent of the planetary mass. Instead of a weaker signal, the microlensing signals of low-mass planets have a shorter duration and a lower detection probability than those of high-mass planets. This means that a microlensing survey with frequent observations of a very large number of stars will be able to detect terrestrial planets at high signal-to-noise (Tytler 1996; Bennett & Rhie 1996; Wambsganss 1997; Bennett & Rhie 2000). The microlensing technique employs stars in the Galactic bulge which act as sources of light rays which are bent by the gravitational fields of stars in the foreground: on the near side of the Galactic bulge, or in the disk. Planets which may orbit these "lens" stars can be detected when the light rays from one of the lensed images pass close to a planet orbiting the lens star. The gravitational field of the planet distorts this lensed image causing a significant variation of the gravitational microlensing light curve from the standard single lens light curve. This planetary deviation is typically of order $\sim 10\%$, and it has a duration of a few hours to a day compared to the typical 1-2 month duration for lensing events due to stars.

The main challenge for a microlensing planet search project is that microlensing events are rare. Only about 3×10^{-6} of Galactic bulge stars are microlensed at any given time (Udalski et al. 1994; Alcock et al. 1997; Alcock et al. 2000), and only $\sim$ 2% of earth-mass planets orbiting these stars will be in the right position to be detected (Bennett & Rhie 1996). The sensitivity limit of the gravitational microlensing technique is set by the finite angular size of the source stars because a very low mass planet will only deflect the light rays from a fraction of the source star's disk. This can wash out the photometric signal of the planet. For main sequence source stars in the Galactic bulge, the sensitivity limit is about $0.1\mathrm{M}_\oplus$, but for giant source stars, it is $> 1\mathrm{M}_\oplus$. Thus, a gravitational microlensing search for terrestrial planets must use main sequence source stars. However, the density of bright main sequence stars in the central Galactic bulge is several stars per square arc second, so angular resolution of $\ll 1$ arc sec is necessary to resolve these stars.

In order to accurately characterize the parameters of the planets discovered via microlensing (Gaudi & Gould 1997; Gaudi 1998), we must have photometry of $\sim 1\%$ accuracy sampled several times per hour over a period of several days (*i.e.* a factor of a few longer than the planetary light curve deviation). The microlensing event light curves must also be sampled continuously for periods of more than 24 hours, in order to unambiguously characterize the planetary signals in microlensing light curves. This allows both the full planetary deviation as well as the periods before and after it to be observed. While it is possible to obtain such accurate photometry for bright source stars (Albrow et al. 2000b; Rhie et al. 2000a) from the ground, this is only useful for microlensing planet search programs which aim to detect giant planets. The vast majority of bright source stars which allow accurate photometry from the ground are giant stars, which have angular sizes that are too large for an efficient terrestrial planet search. For main sequence source stars, the severe stellar crowding in the central Galactic bulge makes it impossible to obtain the required photometric accuracy from ground based observations over a 24 hour period. The Galactic bulge is simply not visible for 24 hour periods from sites with good atmospheric seeing.

1.1. The GEST Mission

It is possible to measure the abundance of Earth-like planets with a gravitational microlensing survey from space, where high angular resolution and photometric stability allow large numbers of main sequence stars to be monitored with the requisite photometric accuracy. Such a mission, known as the the Galactic Exoplanet Survey Telescope,[1] or GEST, has recently been proposed to NASA's Discovery Program, and out simulation is based upon the proposed GEST parameters. The GEST proposal calls for a space-based 1.5m telescope which images 2.1 square degrees of the central Galactic bulge continuously for 8 months per year for a baseline mission duration of three years. GEST would operate from a nearly circular geosynchronous orbit which is inclined by 28.7° (the latitude of Cape Canaveral) from the equator and by $\sim 50^\circ$ with respect to the ecliptic plane. This orbit allows both a continuous view of the central Galactic bulge for eight months per year and a continuous data downlink to a dedicated ground station in the contiguous United States. The GEST camera will contain 62 2048×4608 Marconi CCD42-90 CCDs for a total of 5.9×10^8 pixels. It is anticipated that GEST will take 100 second exposures at 2 minute intervals for a data downlink rate of 70 Mbits/sec (assuming digitization at 14 bits/pixel).

The GEST instrument will be mounted on a Lockheed LM-900 spacecraft which can achieve better than 0.021" pointing stability in GEST's high Earth orbit. GEST will observe a single Galactic bulge field continuously for each eight month Galactic bulge season. This field is located at Galactic coordinates, $l \approx 1.2^\circ$, $b \approx -2.4^\circ$, which is the field closest to the Galactic center which has only a modest amount of extinction. The only variation of GEST's pointing during the eight month Galactic bulge season would

[1] More information on the Galactic Exoplanet Survey Telescope is available at `http://bustard.phys.nd.edu/GEST/`

be a sub-pixel scale dither pattern needed to ensure that the photometric accuracy remains very close to the photon noise limit (Lauer 1999; Gilliland et al. 2000).

GEST will survey $\gtrsim 10^8$ main sequence stars in its selected field, and as our simulation results show, GEST will be sensitive to planets with masses down to $0.1\mathrm{M}_\oplus$, which is 1000 times smaller than the Jupiter and Saturn mass planets probed by the radial velocity technique. If Earth-mass planets are common, our simulations show that GEST will detect about 100 Earth-mass planets. GEST's results will come quickly enough so that measurements of the abundance of terrestrial planets will be available prior to the start of the Terrestrial Planet Finder (TPF) mission in fulfillment of a key recommendation of the McKee-Taylor Decadal Survey Committee (McKee & Taylor 2000).

In this paper, we present the results of a detailed simulation of the GEST mission. In section 2, we explain the assumptions and the details of our simulation and argue that our assumptions are conservative. In section 3, we present the details of our results including example GEST light curves, GEST's predicted planet detection sensitivity, GEST's sensitivity to free-floating planets, and the prospects for direct observations of the lens stars. There is also a brief discussion of the $\sim 50,000$ planets that GEST is likely to detect via transits. Finally, in section 4, we summarize the scientific results to be expected from GEST.

2. The GEST Simulation

In order to simulate the GEST mission, we must make assumptions regarding the source stars, the lens star systems and the GEST telescope. Our distribution of source stars is based upon the Galactic bulge luminosity function of Holtzman et al. (1998). GEST will observe a field at Galactic coordinates $l \approx 1.2^\circ$, $b \approx -2.4^\circ$, which is closer to the Galactic Center than the Baade's window field observed by Holtzman et al. This implies that both the star density and the reddening will be higher, and we split the field into two pieces for the purposes or our simulations in order to account for the gradient of the star density with Galactic latitude. The two half-fields have central Galactic latitudes of $b = -2.0^\circ$ and -2.8°, and we have assigned them star densities of 2.06 and 1.55 times the Holtzman et al. (1998) star density measured at $b = -3.9^\circ$ based upon number counts of "red clump" stars in the MACHO fields (Popowski et al. 2000). The reddenings for these two half fields are assumed to be $A_I = 1.6$ for the inner half field and $A_I = 1.5$ for the outer half field. These reddening values can be obtained from the Schlegel, Finkbeiner & Davis (1998) dust map with a correction for stellar emission as advocated by Stanek (1999) or by assuming that the excess IR emission is proportional to the "red clump" star number counts.

Another very crucial physical input for our simulation is the microlensing probability (or optical depth, τ) towards the Galactic bulge. Measured values are $\tau = 3.3 \pm 1.2 \times 10^{-6}$ at $l = 0.9^\circ$, $b = -3.8^\circ$ (Udalski et al. 1994), $\tau = 3.9^{+1.8}_{-1.2} \times 10^{-6}$ at $l = 2.55^\circ$ and $b = -3.64^\circ$ (Alcock et al. 1997), and $\tau = 3.23^{+0.52}_{0.50} \times 10^{-6}$ at $l = 2.68^\circ$ and $b = -3.35^\circ$ (Alcock et al. 2000). We have used this latest measurement because it is based upon the largest sample, and it is closest to the theoretical estimates. Theoretical determinations of the scaling of the microlensing probability with position Bissantz et al. 1997; Peale 1998 indicate that the microlensing probability at GEST's outer half field ($l = 1.2^\circ$, $b = -2.8^\circ$) should be 1.2-1.3 times larger than at $l = 2.68^\circ$, $b = -3.35^\circ$, while the increase at the inner half field ($l = 1.2^\circ$, $b = -2.0^\circ$) should be a factor 1.4-1.8. For the purposes of this simulation, we have selected a conservative choice for the microlensing probability, $\tau = 2.43 \times 10^{-6}$ at $l = 2.68^\circ$ and $b = -3.35^\circ$ which we then scale to $\tau = 2.9 \times 10^{-6}$ at $l = 1.2^\circ$, $b = -2.8^\circ$, and $\tau = 3.9 \times 10^{-6}$ at $l = 1.2^\circ$, $b = -2.0^\circ$. This is the 1.6σ lower limit on the value of τ extrapolated to our selected field.

The mass function of the lens stars is assumed to follow the a conventional power law form, $f(m) \propto m^{-\alpha}$ where $f(m)dm$ is the number of stars in the mass interval m to $m + dm$. We use a mass function

similar to those advocated by Zoccali et al. (2000) and Kroupa (2000) which imply different values of α in different mass intervals: $\alpha = 2.3$ for $m > 0.8\mathrm{M}_\odot$, $\alpha = 1.33$ for $0.15\mathrm{M}_\odot < \mathrm{m} < 0.8\mathrm{M}_\odot$, and $\alpha = 0.3$, for $0.05\mathrm{M}_\odot < \mathrm{m} < 0.15\mathrm{M}_\odot$. The mass function is truncated at $0.05\mathrm{M}_\odot$ in order to keep the distribution of timescales consistent with the observations of Alcock et al. (2000). Stellar remnants are also included with white dwarfs contributing 13% of the lens stars, while neutron stars and black holes contribute $< 1\%$ and $< 0.1\%$ of the lens stars, respectively.

With these parameters for the properties of the inner Galaxy, we precede to run our simulations as follows:

1. We create an artificial image with stars $0 \leq M_I \leq 9$ at random locations in an artificial image using a "pseudo-gaussian" profile (as in DOPHOT (Schechter, Mateo & Saha 1993)) with a FWHM of 0.25." Brighter stars are not included, but we assume that 5% of GEST's 2.1 square degree field of view is lost due to bright, saturated stars or CCD defects.

2. A stellar lensing event is selected for each star in the frame with lens parameters selected at random assuming the mass function described above and a density and velocity distribution from a standard model of the Galaxy (Han & Gould 1997). All stellar lensing events are assumed to have an impact parameter of ≤ 2 Einstein radii, and the source stars are assumed to reside at 0.5 kpc behind the Galactic Center which is at $R_0 = 8$ kpc.

3. The orientation of each "exo-ecliptic" plane is selected at random, and then planet locations are selected by assigning each planet a random orbital phase within this plane. The planets are assumed to follow circular orbits with radii between 0.25 and 30 AU and mass fractions ranging from $\epsilon = 3 \times 10^{-7}$ to $\epsilon = 10^{-3}$.

4. Planetary lensing light curves are constructed assuming measurements every ten minutes. Finite source effects are incorporated assuming a mass radius relationship taken from Bertelli et al. (1994).

5. The GEST camera is assumed to detect 16 photons per second from an $I = 22$ star, as expected using QE curves for Marconi space qualified CCDs with a 600-1000nm passband.

6. Light curve error bars are generated under the assumption that the photometric accuracy is limited by photon statistics for noise levels down to 0.3%. This level of accuracy has been demonstrated with highly undersampled HST images of very crowded star fields (Lauer 1999; Gilliland et al. 2000). In addition to the source star, the lens star and nearby stars with images that are blended with the source star contribute to the photon noise.

7. A signal-to-noise ratio of 90 is assumed for a ten minute exposure of an isolated $I = 22$ star. This can be achieved with a 600-1000nm passband using space qualified CCDs from vendors such as Marconi or SITe.

8. A single lens, point source light curve is fit to each event, and planet detections are signaled by an excess fit χ^2. We measure the planetary signal with the $\Delta\chi^2$ which is the difference between the χ^2 for the single lens fit and the correct planetary lensing fit. Our detection threshold is $\Delta\chi^2 \geq 160$ which is the equivalent of a 12.5σ detection.

One potential drawback with our method for identifying planet detections is that planet detections may be incorrectly indicated for events with very high magnification because the effects of the finite angular size of the source star may be seen. These high magnification events also have higher sensitivity to planets than lower magnification events (Griest & Safizadeh 1998) because the source star must necessarily pass close to the "stellar" caustic curve which will be distorted due to the presence of planets. However, the determination of the planetary mass fraction (ϵ) and separation can be difficult for events detected due

to the stellar caustic (Dominik 1999). Thus, it is not yet clear how useful such detections will be, although they do present enhanced sensitivity to multiple planets (Gaudi, Naber & Sackett 1998). Because of this uncertainty, we have excluded planets detected in events with maximum magnifications > 200.

3. Expected GEST Results

3.1. Planetary Parameters from Microlensing

The diversity of microlensing planetary light curves has been studied quite extensively (Mao & Paczynski 1991; Gould & Loeb 1992; Bolatto & Falco 1994; Bennett & Rhie 1996; Wambsganss 1997; Gaudi & Gould 1997; Gaudi 1998), and these studies have shown that it is possible to measure both the planetary mass fraction, ϵ, and the planet-star separation from the light curve shape. The duration of the planetary light curve deviation gives ϵ. The overall magnification of the light curve at the time of the planetary deviation and the basic shape of the planetary deviation give the separation. However, the transverse separation, a, is only determined in units of the Einstein ring radius,

$$R_E = 2.85\,\mathrm{AU}\,\sqrt{\frac{M}{\mathrm{M}_\odot}\frac{D}{1\,\mathrm{kpc}}}\,, \qquad (1)$$

which is just the radius of ring image for a single lens of mass M that is perfectly aligned with the source star. $D = D_l(D_s - D_l)/D_l$, where D_l and D_s are the distances to the lens and source stars, respectively.

For a source star in the Galactic bulge, R_E is typically $\sim 2\,$AU, and it ranges from 1-4 AU, so a measurement of a/R_E will yield an estimate of a that is good to a factor of 2. For most of the terrestrial planet detections, however, we can do somewhat better than this because we can also measure the time for the lens center-of-mass to cross the source star radius, t_s. This parameter is measurable for events in which the source comes very close to or crosses one of the lens caustics. This occurs for a large fraction of the terrestrial planet events, but there are many of the giant planet lensing events that are detectable without a close approach to a caustic. Precise values of a and M can be obtained for events in which the lens can be detected either via spectroscopy or proper motion, as the lens separates from the source in the years after the event. This will certainly be possible for the 20% of events in which the lens is brighter than the source, and it is likely to be possible for an additional 20% of events in which the lens is within two magnitudes of the source brightness as discussed below. (See subsection 3.5 for a more detailed discussion of source star identification.)

3.2. Event Light Curves

Examples of the planetary light curves from our GEST simulation are shown in Figures 1 and 2. The data are shown with the error bars determined as described above, and most of the light curves are presented with the sampling interval of 10 minutes that was used for the event detection calculations. While the error bars are meant to indicate the $1\,\sigma$ uncertainties, we have not added this noise to the data points shown in Figures 1 and 2 because of the high density of data points in these figures. These light curves are meant to illustrate the range of planetary light curves that GEST should detect. They also represent the range of signal-to-noise of the terrestrial planet detections in our GEST simulations. Figure 1(a) represents one of the highest signal-to-noise planet detections with the Earth:Sun mass ratio of $\epsilon = 3 \times 10^{-6}$, and Figure 1(b) is an event which barely passes our event detection cut of $\Delta\chi^2 \geq 160$. The other events have more typical signal-to-noise.

We've assumed that GEST's photometric accuracy will be dominated by photon statistics and that systematic errors will not become dominant until the statistical errors reach $< 0.3\%$ (in 5 co-added 100 sec exposures). However, Figures 1 and 2 illustrate that most of the planet detections are made with lower precision photometry. The events shown in Figures 1(a), 1(c), and 2(a) have photometric errors $\gtrsim 1.5\,\%$. (The event shown in Figure 1(d) is plotted with errors of $\sim 1.5\,\%$, but for this event, we plotted individual exposures at 2 minute intervals rather than the co-added measurements plotted for the other events.)

These events serve to illustrate why ground based

microlensing searches are not effective for the detection of terrestrial planets (Bennett & Rhie 2000; Rhie et al. 2000b). The necessity of using main sequence target stars for a microlensing program to find terrestrial planets means that the accuracy of photometry is compromised by the blending of the source star images. This is true even if the planet search program is limit to the best ground based observing sites such as Paranal (Sackett 1999). This blending with neighboring stars less than an arc second away substantially reduces the photometric signal-to-noise and would make the events shown in Figures 1(b)-(d) undetectable. The event shown in Figure 1(a) would have a large enough signal to be detectable from a ground-based program, but since the planetary deviation lasts for more than 24 hours, it would be poorly sampled from a single site. Follow-up observations from sites at other longitudes would be of little help because the poorer seeing at these sites would make the photometry too noisy to be very useful in characterizing the properties of the detected planet.

Figure 2 shows events in which multiple planets are detected. We've run simulations of "solar-type" planetary systems in which every stellar lens is assumed to have planets with the same mass fractions as the planets in the solar system and with the same separations. Most of the multiple planet detections in our simulations are similar to Figure 2(a) in which both the "Jupiter" and "Saturn" planets are detected. In about 25% of the cases where the "Saturn" planet is detected, the Jupiter planet is also detected. This is a consequence of the fact that Saturn's orbital semi-major axis is only a factor of 1.8 larger than Jupiter's orbital semi-major axis. Such orbits are stable only if they are close to circular, so GEST will be able to provide information on the abundance of giant planets with nearly circular orbits by measuring the frequency of double planet detections and the ratios of their separations. This is important information as giant planets in Jupiter or Saturn-like orbits are thought to be required for the delivery of volatiles, such as water, to the inner planets in the habitable zone (Lunine 2001).

Events in which a terrestrial planet and a "Jupiter" are detected, such as the event shown in Figure 2(b) are more rare. In part, this is because the lower mass of the terrestrial planet means that less of them will be detected, but another factor of is that the ratio of Jupiter's semi-major axis to that of the terrestrial planets is a factor of 3.5-7 rather than the factor of 1.8 ratio between the Jupiter and Saturn orbital distances. Because of this, only 10-15% of the detected terrestrial planets will also have a Jupiter detection, but we would expect ~ 10 such double-planet, giant plus terrestrial planet detections if every planet had a solar system like our own.

3.3. Planet Detection Sensitivity

The major goal of our simulations is to determine the planet detection sensitivity of the GEST mission. GEST's sensitivity to planets orbiting each of the lens stars depends on a large number of factors including the event timescale, the size of the photometric error bars, and the angular size of the source star. So, the simplest way to display GEST's detection sensitivity to is to give the number of expected planet detections under the assumption that each lens star has a planet of a given mass fraction, ϵ, and separation. This is what is plotted in Figure 3. The different curves in this figure are contours of constant numbers of planet discoveries, assuming one planet per star at the given mass fraction and semi-major axis. The locations of the planets in our Solar System are also shown. Each planet name start at the planetary mass fraction of the planet and continues toward higher mass fractions. Because the typical mass of a lens star is about $0.3\,\mathrm{M}_\odot$, planets of the same mass as the Solar System's planets will have a typical mass fraction that is larger by about a factor of three. A planet of one Earth mass, for example, will usually have $\epsilon \approx 10^{-5}$ rather than $\epsilon = 3 \times 10^{-6}$, which is the Earth's mass fraction. So, the sensitivity to planets with the same mass as those in the Solar System will appear near the top of each planet name while the bottom of each planet name indicates the sensitivity to planets of a fixed mass fraction. The sensitivity of planets of $1\,\mathrm{M}_\oplus$ is shown in Figure 4 which indicates that just over 100 Earths would be

detected if each lens star has one in a 1 AU orbit. The peak sensitivity is at and orbital distance of 2.5 AU where we would expect 230 detections if each lens star star had a planet in such an orbit.

The green and yellow shaded regions in Figure 3 indicate the sensitivity of other planet search techniques. The known extra-solar planets which orbit main sequence stars have been discovered with the precision radial velocity technique (Marcy & Butler 1996), and a number of these individual detections are indicated in the upper left region of the figure at small semi-major axes and large masses. The solid yellow shaded region indicates the sensitivity of a 20-year radial velocity program assuming a minimum detectable velocity amplitude of $10\mathrm{m/sec}$. This is close to the demonstrated accuracy of the Keck (Marcy & Butler 1996) and CORALIE (Queloz et al. 2000) radial velocity programs, but it is expected that the current radial velocity state of the art is close to the limit set by the intrinsic radial velocity noise of the source stars. The expected sensitivity of the planned 5-year Space Interferometry Mission (SIM) satellite is shown in green with the vertical green lines showing the planned SIM sensitivity and the solid green region showing the sensitivity of the SIM floor mission. (The assumed detectable astrometric signals are 1 μas and 6 μas, respectively, at a distance of 10 pc.)

Figure 3 indicates that GEST has its peak sensitivity at 2-3 AU with significant sensitivity in the range 0.7-10 AU. In fact, the sensitivity at large distances is underestimated by our simulation because we do not consider planets that may be detected when the source star magnification is $A < 1.06$. Events with $A_{\max} < 1.06$ and events with the planetary deviation which occurs before or after the $A > 1.06$ region of the light curve have not been included in our simulations. However, some of these planets will be detectable. A lower limit on our sensitivity to distant planets is set by our sensitivity to free-floating planets which is discussed in section 3.4. This sensitivity is indicated by the thinner, horizontal lines on the right side of Figure 3. These lines should be considered to extend to infinite distances, indicating that GEST has strong sensitivity to the microlensing detection of planets at separations of 0.7 AU to ∞. However, for planets at distances $\gg 10$ AU, it will often be the case that the star that the planet orbits will not be detectable. Such cases may be difficult to distinguish from free-floating planet detections unless the lens star can be detected with follow-up observations (see Section 3.5).

Microlensing of Galactic bulge stars is most sensitive at semi-major axes of 2-3 AU because this is the typical Einstein ring radius for Galactic bulge source stars. Images are located close to the Einstein ring when they are bright, and the a planet is most easily detectable if one of the bright images passes close to it. In contrast, the astrometry technique is more sensitive at large orbital radii, while the radial velocity and transit techniques (see section 3.7) are more sensitive at smaller radii. One difficulty with the astrometry and radial velocity techniques is that planets must be followed for nearly a full orbit for a secure detection (unless the signal is quite large). This is the reason for the change in the slope of the change in the slope of the sensitivity curves for the radial velocity and transit methods at large semi-major axes in Figure 3. Thus, microlensing maintains some advantage over these other techniques at large orbital distances, since it is able to make prompt discoveries of distant planets.

The main advantage of the microlensing technique over both the astrometry and radial velocity techniques is its sensitivity to lower mass planets. At 1 AU, microlensing is sensitive to planets with masses that are about three orders of magnitude smaller than the smallest masses that ground based radial velocity and astrometry searches are likely to detect. A space based microlensing survey also offers an advantage in sensitivity to low mass planets with respect to space based astrometry missions such as SIM. Figure 3 indicates that GEST's sensitivity extends to masses that are a factor of 20 lower than expected for the SIM baseline mission and a factor of 100 lower than for the SIM floor mission. Also, the microlensing results would be likely to come much earlier than the space-based astrometry results. The

GEST mission could be launched as early as 2006, while SIM is not expected to launch before 2009 or 2010. The first microlensing results should come within 6 months or so of launch, but the low mass planet results from SIM are not likely to come before the end of the mission in ~ 2015 when the final astrometric solutions are computed. Thus, GEST appears to have a quite substantial advantage over other planned extra-solar planet detection programs for the study of the abundance of low mass planets. Of course, SIM will find planets orbiting nearby stars, so planetary results to be expected from the GEST and SIM missions are somewhat complementary: GEST will determine extra-solar planet abundances extending down to very low masses, while SIM will study planetary systems close to the Sun with sensitivity down to planets somewhat more massive than the Earth.

Another important advantage of the gravitational microlensing technique is that the low mass planets are detected with high signal-to-noise. In fact, for a large range of planetary masses, the strength of the microlensing signal does not depend on the mass of the planet. Low mass planets do affect a smaller region of the lens plane, so they have a lower detection probability and a shorter duration. Figure 5 shows the distribution of the signal-to-noise of our detected planets for planetary mass fractions ranging from $\epsilon = 3 \times 10^{-7}$ (Mars-like) to $\epsilon = 3 \times 10^{-4}$ (Saturn-like). $\Delta\chi^2$ is the detection significance parameter used for the x-axis of this plot, and a logarithmic scale must be used because of the large spread in $\Delta\chi^2$ values. The most striking feature of this figure is that number of events with large $\Delta\chi^2$ values falls off rather slowly. The power law, $N \sim \left(\Delta\chi^2\right)^{-1.3}$, provides a rough fit to these curves for all but the lowest mass fraction ($\epsilon = 3 \times 10^{-7}$) where the effects of the finite angular size of the source stars begin to reduce the number of high signal-to-noise events.

3.4. Free Floating Planets

The leading theories of planet formation (Levison et al. 1998; Perryman 2000) indicate that planets often don't stay in the same orbit where they formed. The migration of giant planets inward is thought to be necessary to explain the "hot Jupiter" planets discovered by the radial velocity planet searches, and the orbital distribution of Kuiper Belt Objects (Malhotra, Duncan & Levison 2000) suggests that Neptune has migrated outward from its birth site. These migrations are likely to be due to the gravitational interactions of these giant planets with a large number of planetesimals in the protoplanetary disk. Many of these planetesimals are likely to be perturbed into highly elliptical orbits which will send them crashing into the Sun or ejecting them from the solar system, and it is expected that the most massive of these ejected objects will have a mass in the terrestrial planet range which means that they should be detectable via microlensing.

The majority of known extra-solar giant planets in orbits of semi-major axis $> 0.3\,\mathrm{AU}$ have relatively large orbital eccentricities, and this can be explained via gravitational scattering with other giant planets in the same system (Levison et al. 1998). A consequence of these interactions is that many of these giant planets will be ejected from their planetary system. Thus, there are good theoretical reasons to believe that free-floating planets may be abundant as a by-product of the planetary formation process. If so, they can be detected via gravitational microlensing. Figure 6 shows the number of free-floating planet detections expected for the GEST mission under the assumption that there is one free-floating planet per Galactic star. The detection threshold is set higher for the free-floating planet detections because we must search $\sim 10^8$ light curves for free-floating planets while we only need to search the $\sim 10^4$ detected stellar microlensing event light curves for evidence of bound planets. Since theory predicts that many stars may be ejected from the system during the planetary formation process, it may be reasonable to assume that there will be many more free-floating planets than the numbers indicated in Figure 6 (~ 30 planets at $1\,\mathrm{M}_\oplus$). In fact, there has already been a possible detection of a free-floating planet in the MACHO data (Bennett et al. 1997).

3.5. Source Star Identification

Gravitational microlensing is unique among extra-solar planet search techniques in that extra-solar planets can be detected without detecting a significant amount of light from the star that the planet orbits. This allows the detection of planets orbiting very faint stars, such as those in other galaxies (Covone et al. 2000), but it also means that we have less information about the host stars for the planets detected with the gravitational microlensing method. Fortunately, for the specific case of the GEST mission, it is possible to discover much of this information from follow-up observations. In particular, we propose a series of follow-up IR photometry and spectroscopy using adaptive optics (AO) systems on 8-10m class telescopes such as the Keck, Gemini, LBT, or Subaru telescopes. With adaptive optics, at a wavelength of $\leq 2.2\mu$, such a telescope will have seeing of ~ 0.7" or better. This is better angular resolution than GEST will have, and so there should rarely be any difficulty in resolving the source star from its neighbors.

Our simulations indicate that for 20% of the detected planetary events, the lens star will be brighter (in J) than the source star, and for 40% of the detected planetary events, the lens star will be within 2 magnitudes of the brightness of the source star (in the infrared J band). We anticipate that the majority of these lens stars will be detectable with the following procedure: The target stars for the follow-up observations would be selected when planets are detected, and we would take two sets of observations for each target. First, we would get multicolor IR photometry and a moderate resolution IR spectrum of the lensed star before the stellar microlensing event has ended, and then we would repeat the same observations later after the microlensing magnification has ended. This will allow a comparison of the spectra and images with the source star at different magnifications. If we assume a spectral resolution of ~ 2000, then the typical source-lens radial velocity difference of 20-200 km/sec will mean that only a fraction of the source-lens pairs will have lines that are clearly resolved, but the comparison of the of the data taken at different magnifications will allow a clear separation of the spectra of the lens and the source star as long as the lens star is sufficiently bright. When the lens star is detected, it will be possible to determine the masses of the lens star and its planet(s) to $\sim 10\%$ or better.

Another effect that should be detectable in follow-up observations is the proper motion of the lens star with respect to the source. This proper motion is expected to be ~ 3 mas/yr for a typical event, so it should be detectable within a few years for events with relatively bright lens stars. An advantage of proper motion follow-up observations is that observations during the event are not required. This means that it might be possible to do these follow-up observations with NGST.

The lens stars that will be detectable will primarily be G and K-stars which comprise 25% of the lens star population. Our simulations also indicate that 55% of the lens star population will be made up of M-stars, and some of the brightest of these stars should also be detectable. The remaining 20% of lens stars are likely to be white dwarfs and brown dwarfs which would not be detectable.

See Rhie & Bennett (2001) for more details on the follow-up observations.

3.6. Measurable Planetary Parameters

The utility of GEST's planet detections depends, of course, on the properties of the planets that can be measured. These are summarized here:

- The planetary mass fraction, $\epsilon = M_{\rm planet}/M_*$, is always measured. The stellar mass, $M*$, can be estimated to a factor of three accuracy from the microlensing event time scale.
- The planet-star separation (in the plane of the sky) is always measured in units of the Einstein ring radius, R_E. The conversion to physical units depends on the event duration and can be done with an accuracy of a factor of two.
- For $\sim 40\%$ of the detected planetary events, the lens star can be detected via IR follow-up

observations. This will allow a mass determination of the lens star and its planet(s) for the G, K and many of the early M lens stars.

- The masses of the free-floating planets must generally be determined from the event time scale only. This can be done to an accuracy of a factor of three for each individual event.

- Many of the $\sim 1\,\mathrm{M}_\oplus$ planets and virtually all of the $\sim 0.1\,\mathrm{M}_\oplus$ planets detected will have caustic crossing features which depend on the ratio of the source star radius to R_E. This will allow a mass estimate with an accuracy of a factor of two for planets orbiting a star or detected as isolated objects.

3.7. Planet Detection via Transits

While the focus of the GEST mission is to find low mass planets via gravitational microlensing, the survey will also be sensitive to giant planets via transits of the $\sim 10^8$ Galactic bulge stars being monitored. Since giant planets like Jupiter have a radius that is about 10% of a solar radius, a transit of a Jupiter-like planet across the Sun will reduce the apparent brightness of the Sun by about 1%. GEST has the sensitivity to detect such a transit of a solar-type Galactic bulge star by a Saturn size planet, and the following simple argument shows that GEST can detect transits of Saturn size planets orbiting fainter main sequence stars, as well. The luminosity and radius of a main sequence star obeys the following approximate relations: $L \propto M^{3.5}$ and $R \propto M$. Since the fractional photometric signal from a transiting planet (of a fixed radius) goes as R^{-2}, the signal-to-noise for a transiting planet scales as $M^{-0.25}$, which is a very weak dependence slightly favoring lower mass stars.

Some of GEST's $\sim 10^8$ target stars will have their photometry degraded by blended images of their close neighbors, and the probability of a transit for a planet at a given orbital distance depends on the stellar radius. We've computed the number of expected transit detections for planets at different orbital distances, and the results are summarized in Table 1. We've assumed a detection threshold of a 6.5σ detection of a planet of Saturn's radius in 5 hours of exposures. This translates into a 9σ detection of a Jupiter sized planet. A crucial ingredient of our transit detection calculation is the inclusion of realistic stellar radii for the source stars, because many of them have a radius that is substantially smaller than the Sun.

Planets with orbital periods longer than 3 years can be detected via transits, but only one transit will be detected per planet. Such transits should have enough signal-to-noise for a significant detection because the transit duration is $\gtrsim 10$ hours, but the period of the planet can only be roughly estimated from the transit duration. Because of the huge number of stars that GEST observes, planets out to $\sim 20\,\mathrm{AU}$ are detectable even though there is only a probability of $\sim 2 \times 10^{-6}$ that such a planet would have its orbit aligned and be at the right orbital phase to transit the source star. This sensitivity to distant planets via transits means that GEST will have a very substantial overlap between the gravitational microlensing and transit extra-solar planet search techniques. At orbital distances of 0.4-20 AU, GEST will be sensitive to giant planets through both methods. This will allow cross-checks to help confirm the planetary interpretation of the transits. Since the transit signal indicates radius rather than mass, some of the transits could be caused by low mass M-dwarfs or brown dwarfs with similar radii, but much larger masses than giant planets. Thus, some form of confirmation is desirable. For example, we might measure the radial velocities of some sub-sample of the candidate planets detected via transits using a moderate resolution multi-object spectrograph. This would not allow us to distinguish between giant planets and low-mass brown dwarfs, but we should detect radial velocity variations for for those stars which are transited by M-dwarfs or high-mass brown dwarfs. This might allow a statistical correction for the non-planetary transits.

With the combined sample of microlensing and transit detections of giant planets, GEST will be able to probe the entire range of giant planet orbital radii: from 0, where the transit technique is very efficient,

to ∞, where microlensing is the only viable technique. Thus, GEST promises a complete survey of giant planets with the combination of the two techniques.

3.8. Additional GEST Results

There are several other of GEST's planet search capabilities that we have not discussed in detail. Planets orbiting a single star of a binary system have been detected via radial velocities (Marcy & Butler 1996), and gravitational microlensing evidence has been presented for a planet orbiting a binary star system (Bennett et al. 1999), although this interpretation remains uncertain (Albrow et al. 2000a) due to incomplete coverage of the microlensing light curve. Yet another possibility is to detect moons orbiting planets that are detected via microlensing. For a system the Earth and Moon, the probability of detecting both the planet and its moon may be substantial because the Earth-moon separation is about the same of the Einstein radius of an Earth-mass planet in the foreground of the Galactic bulge.

GEST should be able to detect all of these types of planetary systems, and in most cases, it should be possible to determine the parameters of such systems. We will investigate these issue in a future paper.

An additional GEST capability that we have not discussed in this paper is the possibility of studying the abundance of planets in external galaxies, such as M31 (Covone et al. 2000). While most of the source stars in M31 will be either poorly resolved or unresolved, it is still possible to detect microlensing events with giant star sources if the microlensing magnification is not too small. Because an M31 planet search follows mostly giant source stars, it will not be very sensitive to terrestrial extra-solar planets, but it should be able to a detect large number of giant planets at a separation of 1-10 AU and measure their abundance as a function of position in the galaxy. Such a search could be carried out as a part of GEST's Participating Scientist Program (PSP) in which GEST devotes about 3 months per year (when the bulge is not observable) to targets selected via a competitive review. An additional month per year is devoted to Kuiper Belt Object (KBO) search which is expected to discover 100,000 new KBOs (Cook et al. 2000).

4. Conclusions

In this paper, we have presented the results of a simulation of the proposed GEST mission, and we have determined the expected planet detection sensitivity as a function of the planetary mass fraction, ϵ, and the orbital semi-major axis. We have found that GEST will be sensitive to planets down to the mass of Mars, which is about 1000 times less than the masses of planets discovered with the radial velocity technique. GEST would be the first mission sensitive to Earth-mass planets, and it would detect ~ 100 of them at an orbital radius of $1\,\mathrm{AU}$ if every star has such a planet.

We have argued that it is generally possible to accurately determine the planetary mass fraction and to determine the projected planet-star separation to an accuracy of a factor of 2. For $\sim 40\,\%$ of the detected planets it should be possible to detect the lens star with adaptive optics observations in the infrared.

The expected scientific output of the GEST planet search programs is summarized here:

- The average number of planets per star down to $0.1\,\mathrm{M}_\oplus$ at separations of $\sim 0.7\,\mathrm{AU}$ - ∞ for terrestrial planets and 0 - ∞ for giant planets.
- The planetary mass function as a function of the planetary mass fraction, $f(M_{\rm planet}/M_*)$, and separation, for all lens stars.
- The planetary mass function as a function of star and planet masses as well as separation for G, K, and early M stars.
- The abundance of giant planet pairs. A high abundance will indicate a large fraction of near circular orbits.
- The ratio of free-floating to bound planets as a function of planetary mass.

Finally, we'd like to emphasize that the results that we've presented are based upon very conservative assumptions. We've assumed a microlensing optical depth number that is 1.3 times smaller than the latest measurements indicate. If we assume that the optical depth measurement errors have a normal distribution, this is the 95% confidence level lower limit on the microlensing optical depth. We also assume a circular field-of-view, but a three-mirror anastigmatic telescope design would allow for a non-circular field-of-view. This allows us to select a Galactic bulge field with a microlensing optical depth that is higher by a factor of about 1.3. Thus, the combination of the best microlensing optical depth measurement and the three-mirror anastigmatic telescope design could increase our expected planetary discovery rate by a factor of 1.7.

We've also been conservative in the selection of our planet selection criteria by demanding a 12.5σ improvement ($\Delta\chi^2 \geq 160$) for a planetary microlensing fit compared to a single lens fit. This ensures that we can make a reasonably accurate determination of the planetary parameters, but we could probably increase our event count by about 70% if we dropped our threshold to 9σ. Furthermore, we've not included events with a peak magnification $A_{\rm max} > 200$ because they may be difficult to interpret. All told, if we dropped all of our conservative assumptions, we would have an event rate that is 3-4 times higher than we have reported (although the interpretation of some of these events might be difficult).

In summary, we've demonstrated that the GEST mission can detect planets with masses down to that of Mars which is some three orders of magnitude less than current techniques. GEST is unique among indirect terrestrial planet search programs in that low mass planets are detected at high signal-to-noise. GEST is sensitive to terrestrial planets at orbital distances of $\gtrsim 0.7\,$AU via microlensing, and it is sensitive to giant planets are all orbital radii because giant planets can be detected via transits. If each star has a $1\,{\rm M}_\oplus$ planet orbiting at $1\,$AU, GEST would detect ~ 100 of these. The results we've presented indicate that GEST could provide very useful statistics on the abundance of terrestrial and giant planets well in advance of the Terrestrial Planet Finder (TPF) mission, and this information would likely be quite useful in planning TPF.

Acknowledgments

We'd like to thank John Mather for encouragement and advice during the early stages of this work, and we'd also like to thank Domenick Tenerelli and his team at Lockheed Martin Space Systems for their efforts on behalf of the GEST Discovery proposal. Finally, we'd like to thank the GEST Co-Investigators for their help. The Co-Investigators are: M. Clampin, K. Cook, A. Drake, A. Gould, K. Horne, S. Horner, D. Jewitt, G. Langston, T. Lauer, A. Lumsdaine, D. Minniti, S. Peale, M. Shao, R. Stevenson, D. Tytler, and N. Woolf. This work was supported, in part, by NASA Grants NAG5-4573 and NAG5-9731.

REFERENCES

Albrow, M. D., et al. 2000a, ApJ, 534, 894.

Albrow, M. D., et al. 2000b, ApJ, 535, 176.

Alcock, C., et al. 1997, ApJ, 479, 119; (E) 500, 522

Alcock, C., et al. 2000, ApJ, 541, 734

Beichman, C. 1998 Terrestrial Planet Finder: The Search for Life-Bearing Planets Around Other Stars SPIE, 3350, 719

Bennett, D. P., et al. 1997, ASP Conf. Proc. 119: Planets Beyond the Solar System and the Next Generation of Space Missions, D.R. Soderblom, ed., p. 95. (astro-ph/9612208)

Bennett, D. P., & Rhie, S. H., 1996, ApJ, 472, 660.

Bennett, D. P., & Rhie, S. H., 2000, Proc. of the Disks, Planetesimals & Planets Meeting held in Tenerife, Jan. 24-28, 2000, (astro-ph/0003102)

Bennett, D. P., et al. 1999, Nature, 402, 57.

Bennett, D. P., et al. 2000, BAAS, vol. 32, no. 3, p. 3206; (also at http://bustard.phys.nd.edu/GEST/publications.html)

Bertelli, G., Bressan, A., Chiosi, C., Fagotto, F., & Nasi, E. 1994, A&AS, 106, 275

Bissantz, N., Englmaier, P., Binney, J., & Gerhard, O., 1997, MNRAS, 289, 651

Bolatto, A. D., & Falco, E. E. 1994, ApJ, 436, 112

Butler, R. P. & Marcy, G. W., 1996, ApJ, 464, L153

Cook, K. H., et al. 2000, BAAS, vol. 32, no. 3, p. 2101; (also at http://bustard.phys.nd.edu/GEST/publications.html)

Covone, G., de Ritis, R., Dominik, M., Marino, A. A., et al. 2000, A&A, 357, 816

Danner R, Unwin S 1999 *SIM: Taking the Measure of the Universe* NASA/JPL

Deeg, H. J., et al. 2000, ASP Conf. Proc., in press: Planetary Systems in the Universe: Observation, Formation and Evolution (IAU Symp. 202), Penny, Artymowicz, Lagrange and Russell, eds. (astro-ph/0011143)

Dominik, M. 1999, A&A, 341, 943

Dressler, A., et al. 1996, "HST and Beyond; Exploration and the Search for Origins: A Vision for Ultraviolet-Optical-Infrared Space Astronomy," AURA publication, available at: http://www.stsci.edu/stsci/org/hst-and-beyond-report.pdf

Fridlund, C.,V., M. 2000 Darwin: the Infrared Space Interferometer in B Schürmann, ed., *Darwin and Astronomy* 11–18 ESA SP–451, Noordwijk, NL

Gaudi, B. S., & Gould, A. 1997, ApJ, 486, 85

Gaudi, B. S., Naber, R. M. & Sackett, P. D. 1998, ApJ, 508, L33

Gaudi, B. S. 1998, ApJ, 506, 533

Gilliland, R. L., et al. 2000, ApJ, in press (astro-ph/0009397)

Gould, A., & Loeb, A. 1992, ApJ, 396, 104

Griest, K. & Safi zadeh, N. 1998, ApJ, 500, 37

Han, C. & Gould, A. 1997, ApJ, 480, 196

Holtzman, J. A., et al. 1998, AJ, 115, 1946

Koch, D. G., et al. 1998, SPIE, 3356, 599

Kroupa, P., & Tout, C. A. 1997, MNRAS, 287, 402

Kroupa, P. 2000, International Conference of the Astronomische Gesellschaft, vol. 16, p. 11

Lauer, T. R. 1999, PASP, 111, 1434

Levison, H. F., Lissauer, J. J., Duncan, M. J. 1998, AJ, 116, 1998

Lunine, J. I. 2001, Proc. Nat. Acad. Sci., submitted.

Malhotra, R., Duncan, M. J. & Levison, H. F. 2000, in Protostars and Planets IV, eds Mannings, V., Boss, A.P., Russell, S. S., p. 1231

McKee, C. F., Taylor, J. H., (eds.) 2000, "Astronomy and Astrophysics in the New Millennium," National Academy Press, Washington, D. C.

Mao, S., & Paczyński, B. 1991, ApJ, 374, L37

Marcy, G. W., & Butler, R. P. 1996, ApJ, 464, L147

Marcy, G. W., & Butler, R. P. 2000, PASP, 112, 137

Marcy, G. W., Cochran, W. & Mayor, M. 2000, in Protostars and Planets IV, eds Mannings, V., Boss, A.P., Russell, S. S., p. 1285

Mayor, M., & Queloz, D. 1995, Nature, 378, 355

Peale, S. J. 1997, Icarus, 127, 269

Peale, S. J. 1998, ApJ, 509, 177

Perryman, M. A. C. 2000, Rep. Prog. Phys., in press (astro-ph/0005602)

Popowski, P., et al. 2000, preprint (astro-ph/0005466)

Queloz, D., et al. 2000, A&A, 354, 99

Rhie, S. H., et al. 2000, ApJ, 533, 378

Rhie, S. H., et al. 2000b, BAAS, vol. 32, no. 3, p. 3210; (also at http://bustard.phys.nd.edu/GEST/publications.html)

Rhie, S. H., & Bennett, D. P., 2001, in preparation

Sackett, P. D., et al. 1999, Planets Outside the Solar System: Theory and Observations, J.-M. Mariotti and D. Alloin, eds., p. 189

Schneider, J., Auvergne, M., Baglin, A., et al. 1998 The COROT Mission: From Structure of Stars to Origin of Planetary Systems in Woodward, Shull, Thronson, eds., *Origins* ASP Conf. Series 148 298–303 San Francisco

Schechter, P. L., Mateo, M. & Saha, A. 1993, PASP, 105, 1342

Schlegel, D. J., Finkbeiner, D. P. & Davis, M. 1998, ApJ, 500, 525

Stanek, K. Z. 1999, ApJ, submitted (astro-ph/9802307)

Tytler, D. 1996, in "A Road Map for the Exploration of Neighboring Planetary Systems (ExNPS)," Chap. 7, available at http://origins.jpl.nasa.gov/library/exnps/ExNPS.html

Udalski, A., Szymanski, M., Kaluzny, J., Kubiak, M., Krzeminski, W., Mateo, M., Preston, G. W., & Paczyński, B. 1994, Acta Astronomica, 44, 165

Wambsganss, T. R. 1997, MNRAS, 284, 172

Zoccali, C., et al. 2000, ApJ, 530, 418

This 2-column preprint was prepared with the AAS LaTeX macros v4.0.

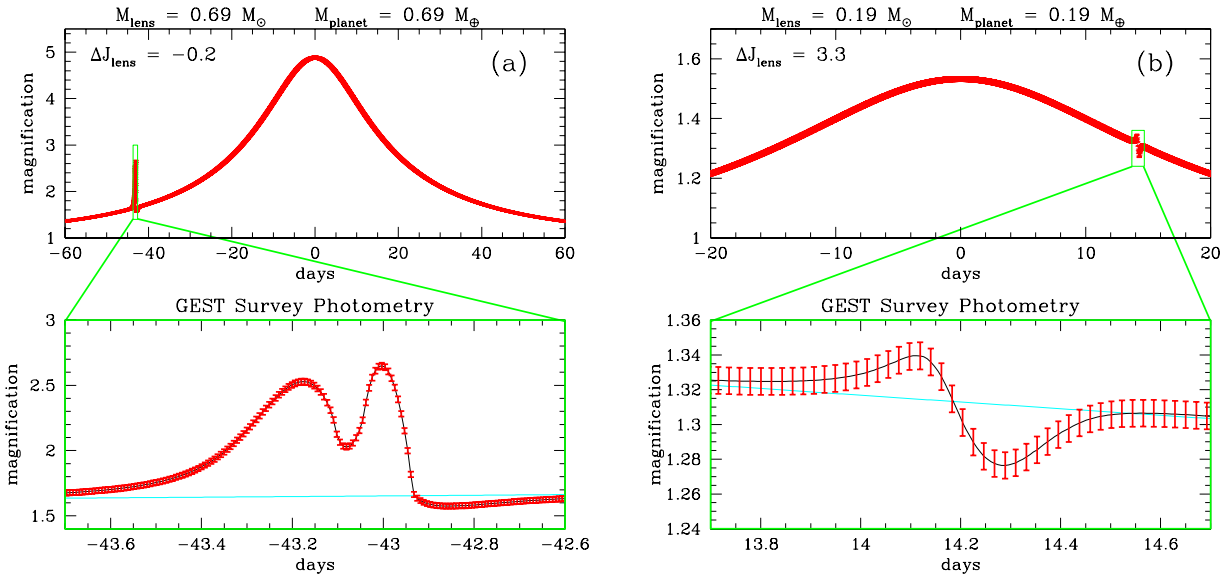

Fig. 1.— Example light curves from a simulation of the GEST mission. In each case, the top panel shows the full light curve, and the planetary deviation region(s), outlined in green, is blown up and shown in the lower panel. All of the example light curves have the Earth:Sun mass ratio of $\epsilon = 3 \times 10^{-6}$. (a) and (b) span the range of planetary detection signifi cance from $\Delta\chi^2 = 60,000$ (a) to $\Delta\chi^2 = 180$ (b) which is just above our cut, while (c) and (d) show more typical light curves with $\Delta\chi^2 = 600 - 1300$. The planets detected in (b) and (c) have orbital radii of 1 AU while the events shown in (a) and (d) have orbital radii of 5 and 2.5 AU, respectively. $\Delta \mathrm{J}_{\mathrm{lens}}$ is the difference between lens and source J magnitude.

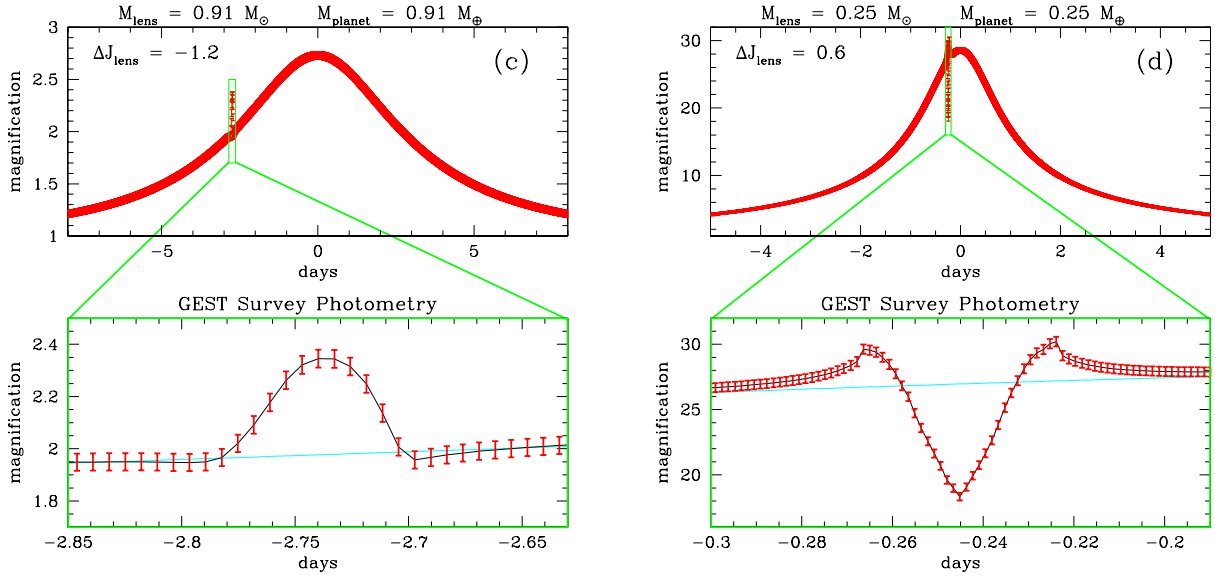

Fig. 1.— continued.

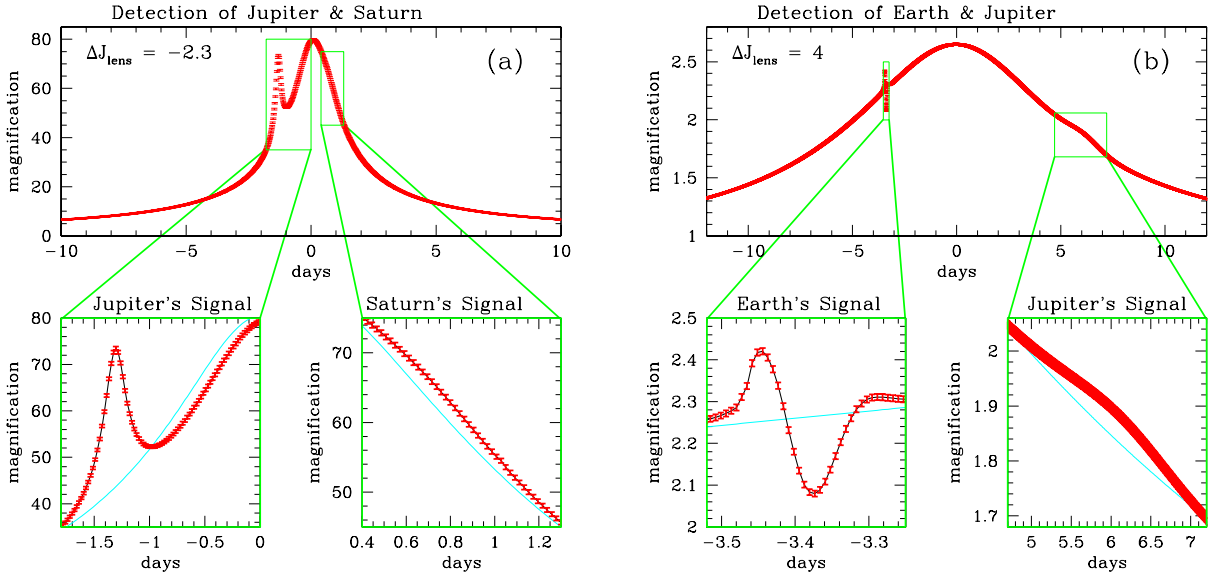

Fig. 2.— Example multiple planet light curves from our simulation of planetary systems with the same planetary mass ratios and separations as in our solar system. (a) is an example of a Jupiter/Saturn detections and (b) is an example of the detection of Earth and a Jupiter.

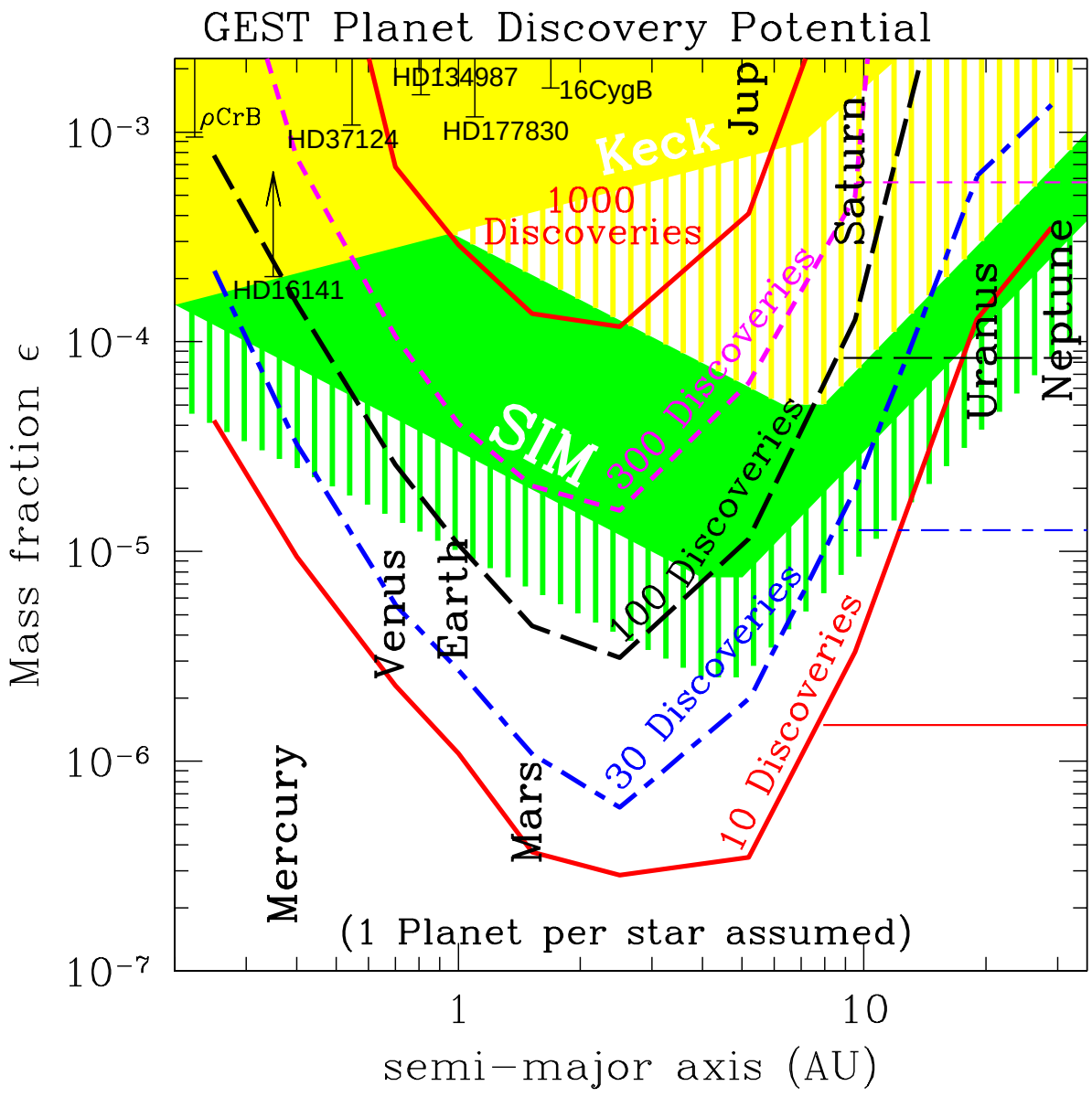

Fig. 3.— The GEST mission sensitivity is plotted as a function of planetary mass fraction, ϵ, and orbital semi-major axis. The curves are contours indicating the expected number of GEST planet discoveries assuming 1 planet per star with the given parameters. The solid yellow region gives the sensitivity of a 20-year radial velocity program on the Keck Telescope assuming a detection threshold of 10 m/sec, and the yellow lines indicate the sensitivity of a 10-year interferometric astrometry program with a 30 μas detection threshold. The green regions indicate the sensitivity of the SIM recommended and floor missions. The location of our Solar System's planets and some of the extra-solar planets detected by radial velocities are shown. Most detected Earth mass planets have $\epsilon \approx 10^{-5}$ because the typical lens star has a mass of $\sim 0.3 M_\odot$, so the plot indicates that GEST can see ~ 35 Earth-mass ratio planets at 1 AU and ~ 100 Earth-mass planets at that distance. The horizontal lines indicate the sensitivity to free-floating planets since the more distant planets can sometimes be detected without seeing a microlensing signal from their star.

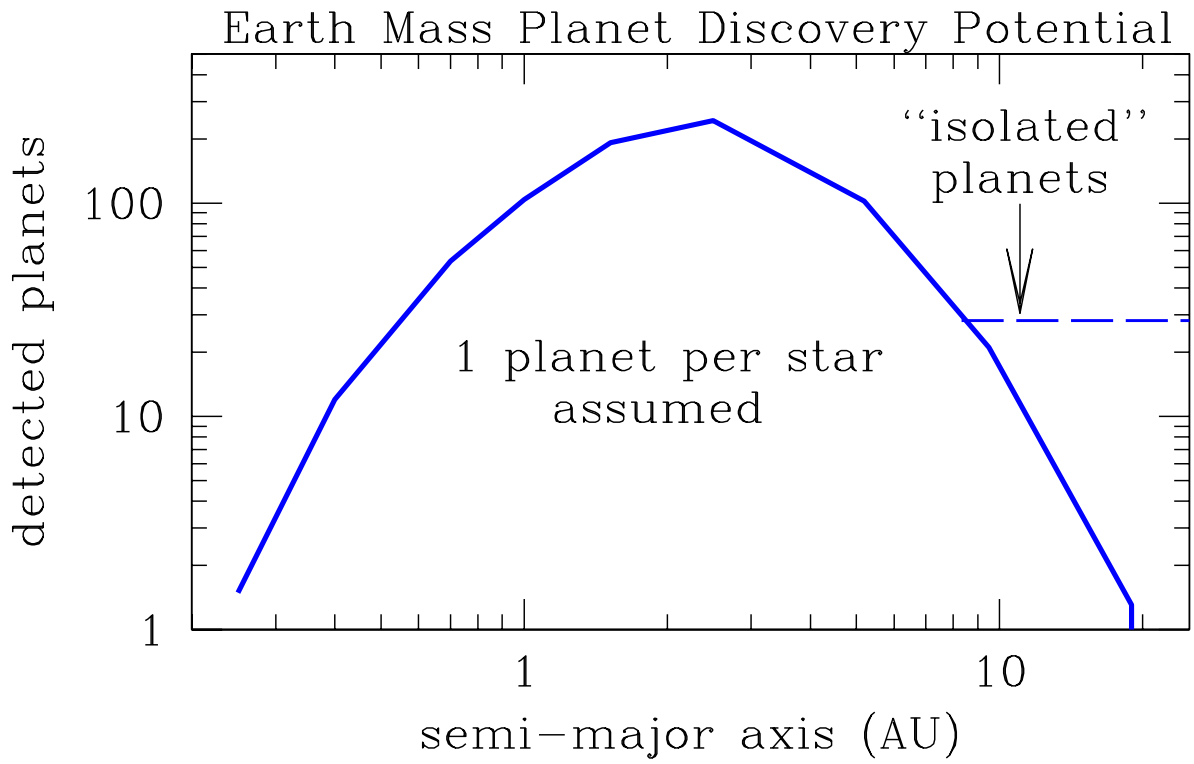

Fig. 4.— This is a plot of GEST's sensitivity to Earth-mass planets. The number of detected Earth-mass planets is shown as a function of the orbital semi-major axis assuming one such planet per lens star. At a semi-major axis of $\sim$ 10 AU, the number of planet detections reaches the lower limit of about 30 set by the free-floating planet detection calculation. Most of the planets detected with semi-major axis $\gg$ 10 AU will be detected in "isolation," without a detection of their host star.

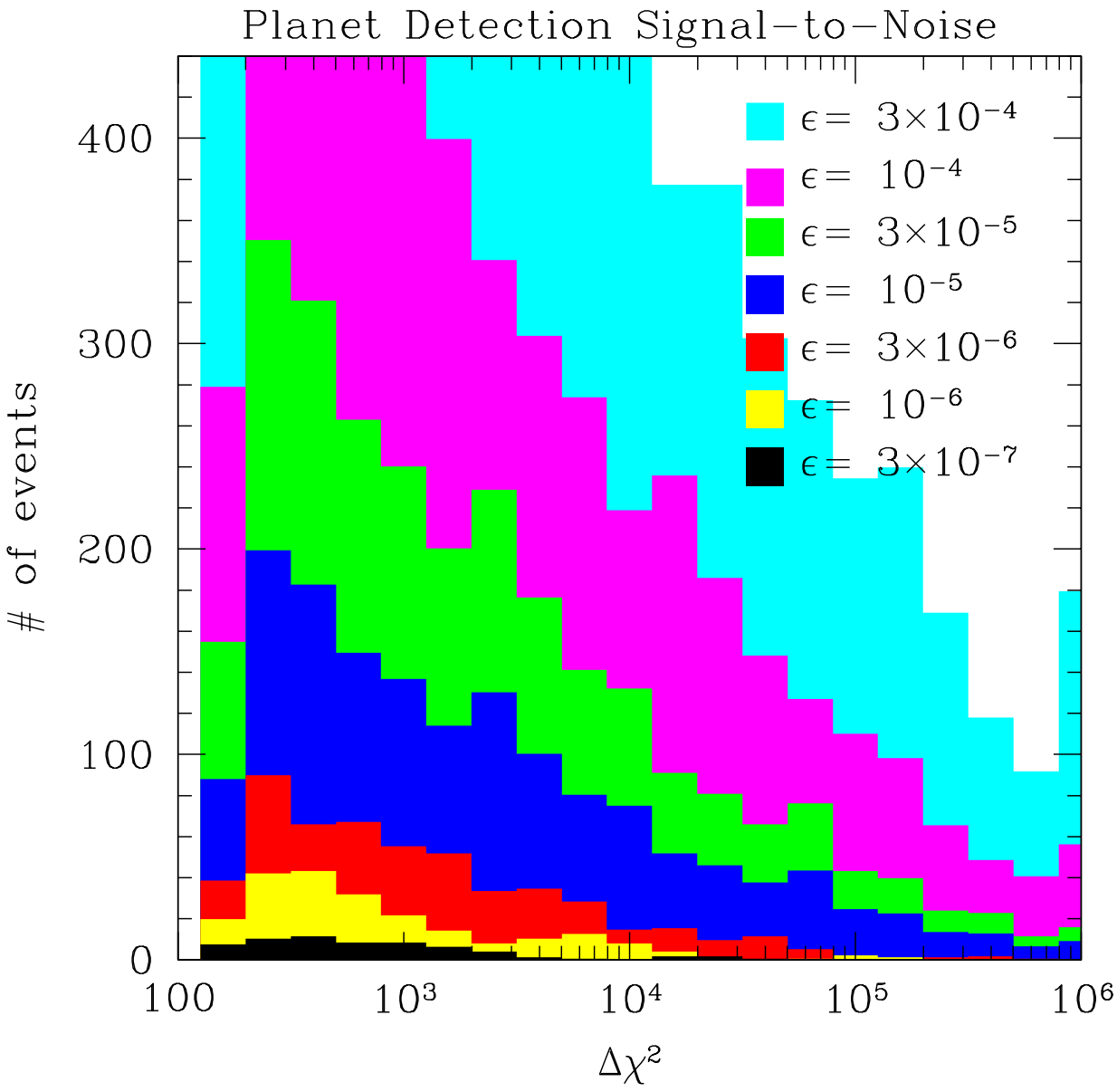

Fig. 5.— This is a histogram of the planetary detection signifi cance, $\Delta\chi^2$, for different mass fractions, ϵ, ranging from $\epsilon = 3 \times 10^{-7}$ (the mass fraction of Mars) to $\epsilon = 3 \times 10^{-4}$ (the mass fraction of Saturn). For planets with an Earth-like mass fraction ($\epsilon = 3 \times 10^{-6}$) and above, more than half of the detected events have $\Delta\chi^2 > 800$ which corresponds to a 28σ detection.

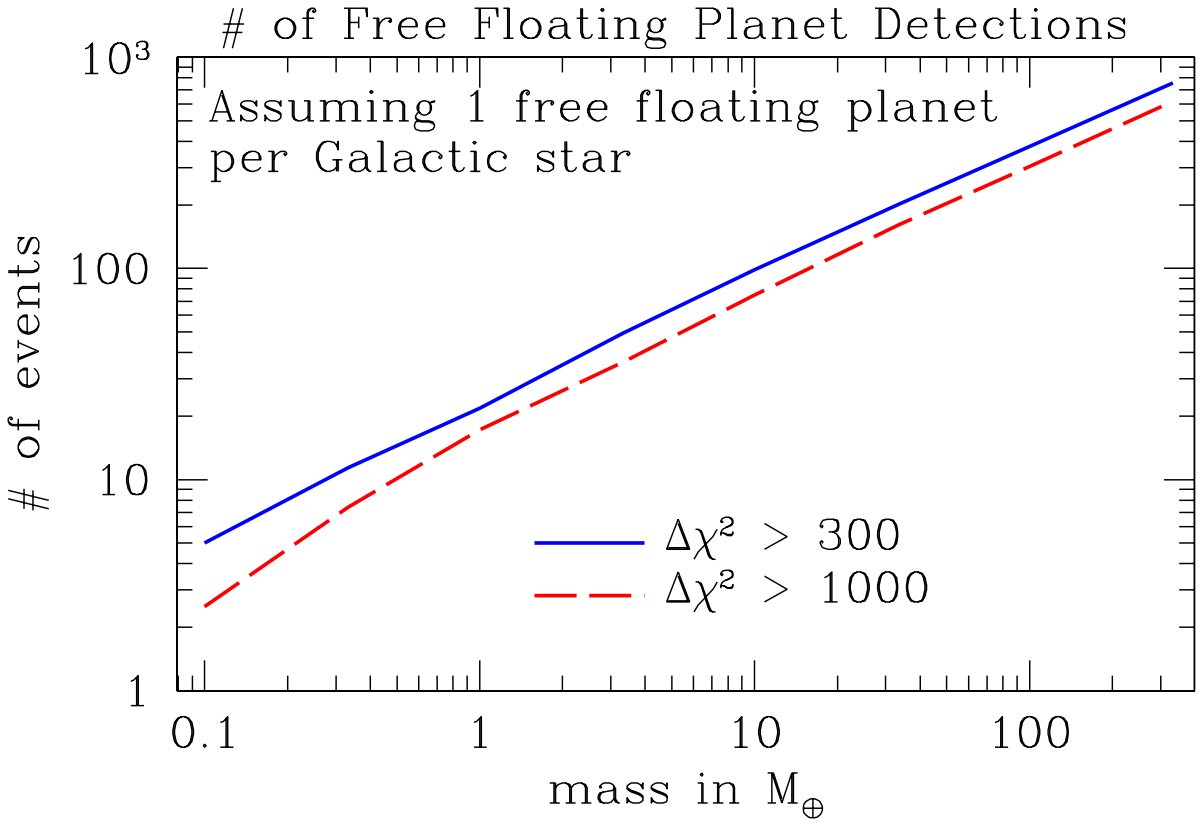

Fig. 6.— The number of free-floating planets to be discovered by GEST vs. planetary mass for 2 different detection criteria which are equivalent to 17σ and 30σ, respectively.

TABLE 1
PLANETARY TRANSITS FROM GEST

Semi-major axis (AU)	Period (yrs.)	# of detections	transits per planet	transit duration
0.04	~ 0.01	5,000,000	~ 200	1.6
0.4	~ 0.3	600,000	~ 7	5
1.0	~ 1.3	160,000	~ 2	8
2.0	~ 3.7	40,000	1	11
5.2	~ 15	6,000	1	18
9.5	~ 40	1,300	1	24
19.5	~ 110	200	1	35

This table shows the number of expected transit planet detections for planets with a radius at least as large as that of Saturn for a three year GEST mission assuming 8 months of observations per year. The planet detection numbers assume 1 planet per star.